

### J3.7 Free Tropospheric Humidity observations from METEOSAT water vapor data

Rémy Roca, H el ene Brogniez, Laurence Picon and Michel Desbois  
LMD,  cole Polytechnique, Palaiseau, 91128, France.

#### 1. INTRODUCTION

Water vapor in the intertropical free troposphere plays an important role on the long wave radiation budget of the tropical climate. It is influenced by tropical deep convection, by the mid-latitudes and the general circulation yielding to features spanning a wide range of scale (e.g. Pierrehumbert and Roca, 1998). The METEOSAT satellites provide 6.3 m radiances measurements continuously since around 20 years offering a unique documentation of the mean water vapor distribution and its variability over Africa and the tropical Atlantic Ocean at a high space and time resolution. In this paper, we present an exploitation of a part of the METEOSAT archive. The raw clear sky signal is inverted in terms of Free Tropospheric Humidity. The algorithm and its validation are first shown using METEOSAT-5 data over the Indian Ocean during the INDOEX campaign. Then recent developments concerning the nominal METEOSAT observations and its homogeneity over the 1983-1994 period are introduced. The retrieval technique is then applied onto the homogenized archive extracted from the ISCCP-B3. The July 1992 climatology is presented as an example of this new product and the cloud clearing technique impacts are discussed.

#### 2. FREE TROPOSPHERIC HUMIDITY (FTH) FROM METEOSAT

While the use of Upper Tropospheric Humidity (UTH) may be adapted for the moist areas, it may be misleading over the whole intertropical region. Figure 1 shows the weighting functions of the METEOSAT-5 6.3 microns captor for a tropical moist case and for a subtropical dry case. With respect to the moist case, the subtropical synthetic profile weighting function peaks slightly lower (375 hPa instead of 300 hPa) and broaden down with normalized contribution up to 20% as low as 700 hPa (550 hPa for the tropical sounding). Given that the radiance is can be

understood in terms of the weighting-function weighted mean relative humidity of the atmospheric column and owing to the

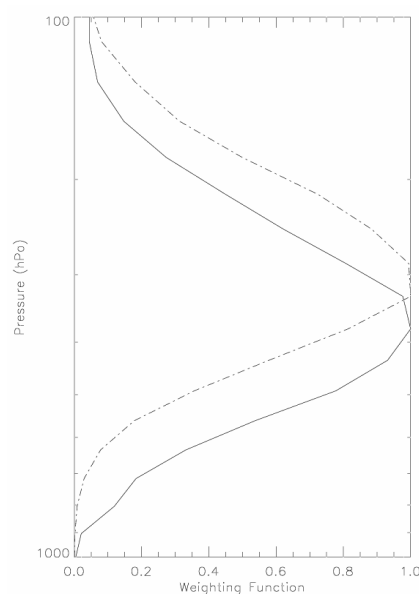


Figure 1 METEOSAT-5 weighting function. Dotted line is for a moist profile (RH=70%) over 800-100 hPa and plain line for a dry profile (RH=20%). In the boundary layer (1000-800 hPa), RH is set to 80%

variability of the weighing function, this parameter will be designed in this paper as the Free Tropospheric Humidity (FTH).

The retrieval algorithm used here was inspired by the EUMETSAT operational UTH algorithm (Schmetz et al., 1995) which is based on the developments of Soden and Bretherton (1993). The algorithm simply links the brightness temperature ( $T_B$ ) to the FTH according to :

$$\ln(p_0 \text{FTH} / \cos \theta) = aT_B + b \quad (1)$$

where  $p_0$  is a temperature vertical distribution normalizing factor equal to the ratio of the 240K isobars to 300 hPa (see Engelen and Stephens, 1998).  $\theta$  is the viewing angle. The coefficients  $a$  and  $b$  are obtained from *local* look-up tables. These LUT are computed using a wide vertical layer (800-100

\* Corresponding author address: R emy Roca, LMD,  cole Polytechnique, 91128 Palaiseau, France; e-mail: roca@lmd.polytechnique.fr

hPa) with constant relative humidity. The radiative transfer simulations are performed using an updated version of an ECMWF radiative code (Morcrette and Fouquart, 1985) which was shown to agree well within 0.5K with the formerly operationally used code of EUMETSAT (Tjemkes et al., 1996; Roca, 2000). This narrow band model includes the filter function of the captor as well as the observing geometry.

The algorithm is evaluated using METEOSAT-5 measurements over the Indian Ocean and an ensemble of 240 radiosondes launched from ships and islands during the INDOEX campaign in winter 1999. Figure 2 shows the scatter diagram of the radiosondes derived

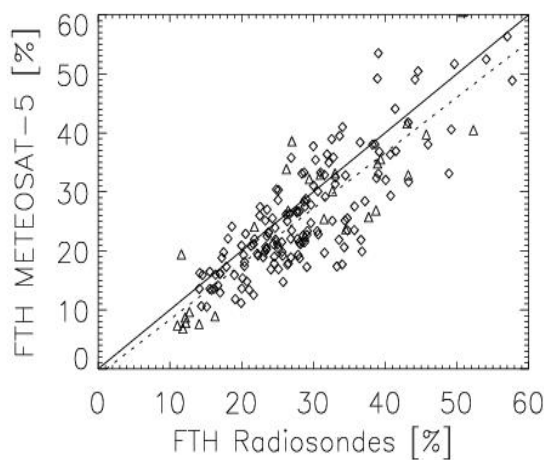


Figure 2 Scatter diagram of satellite derived FTH satellite and radiosondes derived FTH for 240 radiosondes during INDOEX.

FTH versus the satellite derived FTH. The *in-situ* estimates are obtained by first computing the radiosondes weighting functions and then

vertically averaging using the weights. The METEOSAT-retrieved FTH agrees well with the radiosondes derived FTH with a small bias of 2.7% and a standard deviation of 6%. Only the clear sky scenes are retained in the comparisons owing to the availability of a cloud mask which computation is detailed in Roca et al. (2002). Note that in this case, the loop up table are built from the ECMWF operational analysis temperature profiles.

### 3. LONG TERM CALIBRATION ISSUES OF THE METEOSAT ARCHIVE

While the absolute calibration of the METEOSAT-WV channel has been investigated in the literature since a long time (see Bréon et al., 2000 and Tjemkes et al., 2001 for an update), the long term homogeneity of the archive received only few attention. Recently, Picon et al. (2002) proposed a new METEOSAT archive covering the July 1983 to February 1994 period where the data are homogenized in time with respect to the 1994 absolute calibration. Figure 3 shows the mean brightness temperature over the 45°S-45°N, 45°W-45°E region for the above mentioned period from the original dataset and from the corrected one. The corrected archive clearly recovers the previously missing seasonal cycle of 1987. Unlike the original raw data, the corrected data set over the period before 1987 appears to resemble the last part of the time series with similar magnitude and range of the seasonal cycle. While such an approach does not rule out any systematic bias in the absolute calibration, it allows the investigation of the climatology using an homogenous long term data set.

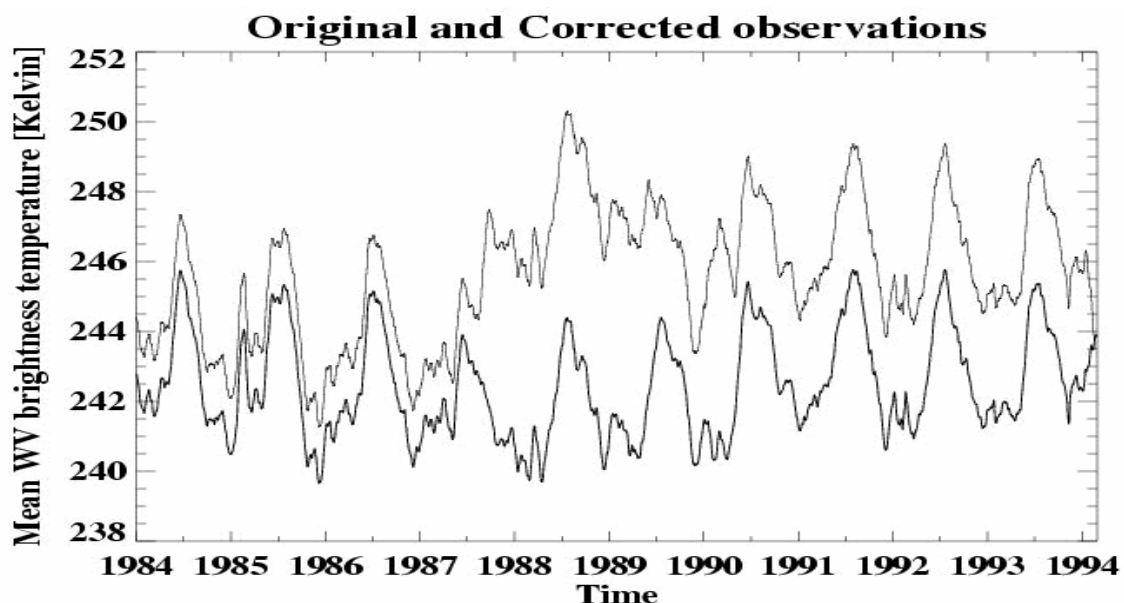


Figure 3: Time series of METEOSAT WV brightness temperature averaged over the tropical Atlantic and Africa. 1-Month running mean. The thin line is for the original archive and the thick line for the corrected one.

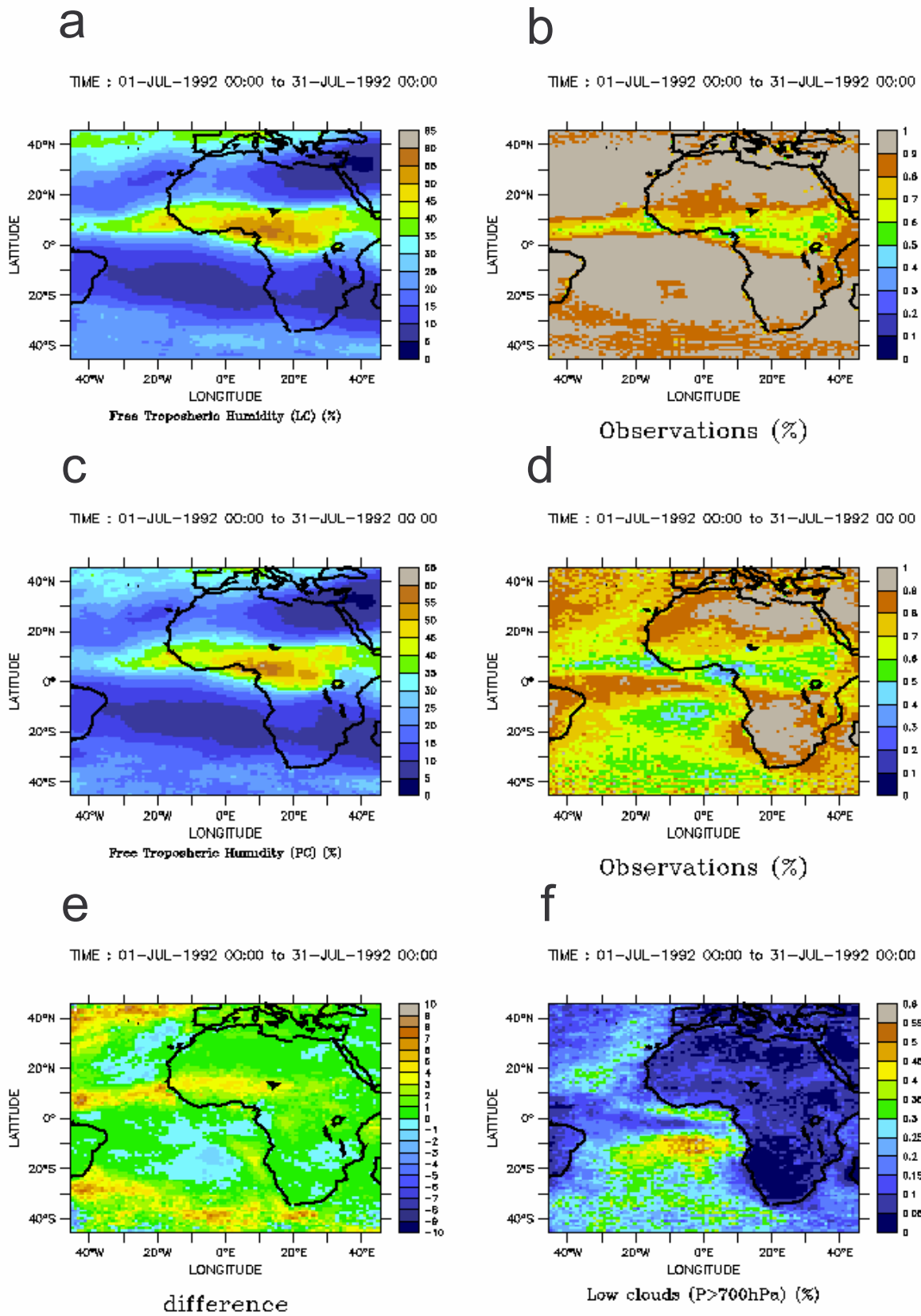


Figure 4 July 1992 maps of FTH (a), FTH pure clear sky (c) and difference (e). Percentage of observations of FTH (b), of FTH pure clear sky (d) and low cloud cover (f).

#### 4. PROCESSING OF THE ARCHIVE

Previous to applying the retrieval, two processing steps are needed: i) cloud clearing and ii) computations of the local look-up tables.

##### 4.1 Cloud clearing

Cloud clearing consists in keeping, during the space/time averaging of the data, only the clear sky scenes where the retrieval can be performed. A first approach could be to filter out all of the pixels for which the column is flagged cloudy by any other either on-board or ancillary cloud detection products hence forming "pure clear sky" FTH. Nevertheless as indicated by Schmetz and Turpeinen (1988), low levels clouds (below 700 hPa) are unlikely to influence the METEOSAT radiances much and such low cloud pixels could be used for the FTH estimation. Figure 1 recalls the main features of the METEOSAT weighting function vertical distribution in the intertropical belt, and suggests that, for instance, trade cumulus at the top of the marine boundary layer at around 850 hPa would hardly be seen by the WV channel, especially in the moist regions. Using an ensemble of synthetic dry profiles similar to the ones used in Figure 1, and considering a black cloud at different altitudes, the radiative impact onto the radiance is computed. The results indicate that for a very dry profile with FTH=2%, a cloud at 700 hPa cools the BT by 1.75K. The cooling is less than 0.25K for FTH=20% and moister. Such cloud effect translates in an absolute error of 0.5% to 1.5% for FTH from 2 to 60%. Hence, a threshold of 700 hPa is conserved.

Cloud information is taken from ISCCP database (Rossow and Garder, 1993). Indeed the so-called DX product provides a number of cloud related information (occurrence, cloud top pressure,...) at the B3 stage pixel level (30km/3hours). This dataset offers a unique source of simultaneous cloud detection results and "water vapor" radiances which spans the whole period 1983-1994 and allows us to cloud clear the whole corrected archive.

##### 4.2 Look up tables computations

In order to establish the local distribution of the regression coefficients for the inversion, the NCEP Reanalysis (Kalney et al., 1996) daily temperature profiles, readily available over our period of interest, are used. Relative humidity is imposed at 5% and 50% constant over the 800-100 hPa range while for the lower

level daily RH from the analysis is used. These two synthetic profiles allows to compute the daily regression coefficients for each  $2.5^{\circ} \times 2.5^{\circ}$  grid points over the studied regions. Similarly, the daily NCEP temperature profiles provide the local estimated value of the  $p_0$  parameter.

The full treatment is currently in process at LMD and we shall highlight here a few of its features for the year 1992. The full climatology will be presented at the conference.

#### 5. THE JULY 1992 CLIMATOLOGY

Figure 4a shows the mean July 1992 FTH distribution over the tropical Atlantic and Africa. The moist ITCZ is evident with FTH around 40-60% as well as the strong subsidence regions in the subtropics with FTH as low as 5% over large areas. Figure 4b shows the percentage of observations used to build the mean FTH. In the ITCZ, 40 to 80% of the observations were kept in the mean while almost all of them are retained in the subtropical dry areas. In order to compare, the same information is presented in Figure 4c and d for the "pure clear sky" FTH. The large scale humidity patterns of the two products closely resembles one another despite the fact that less observations are used to build the "pure clear sky" FTH. For instance, over the strato-cumulus region in the south Atlantic only 20 to 30% of the observations are kept in the seasonal mean. Over the ITCZ, the cloud clearing also allows to increase the number of points for available for the mean (Figure 4d). FTH is overall moister than the "pure clear sky" FTH with excess up to 8-10% in the northern mid-latitudes and west of Senegal. This moist bias could be attributed to the moist free troposphere and low level clouds situation before deep convection develops which are not taken into account in the "pure clear sky" cases. On the other hand, over the edges of the driest spots of the subtropical areas, FTH is dryer than the "pure clear sky" FTH. The absolute difference (Fig. 4e) reaches -1% in the driest areas which translates into a 20 to 50% relative difference due to the dry background. There, the non-cleared pixels could be associated with the driest conditions of strong subsidence capping the otherwise moist and cloudy marine boundary layer. These features deserves further investigations and will be detailed at the conference together with the comparisons with the TOVS derived UTH climatology (Bates et al., 2001).

## 6. CONCLUSIONS

A new METEOSAT archive corrected from its original inhomogeneities is used to compute the climatology of Free Tropospheric Humidity over Africa and the tropical Atlantic Ocean. The algorithm for inverting the raw radiances is shown to agree very well with an ensemble of radiosondes with a small bias of 2.7% and a standard deviation of 6%. The ISCCP pixel level data are used for cloud clarification and following the EUMETSAT approach, only the scene with medium or high clouds are filtered off offering densely observed seasonal means. The present data base has a resolution of  $0.625^{\circ} \times 0.625^{\circ}$ , 3 hours currently covering July 1983-February 1994 and will allow the investigation of the water vapor distribution in the intertropical belt from the mesoscale features to the recent climate variability.

## 7. ACKNOWLEDGMENTS

We thank JL Monge for his support with the new archive data management among other things. The homogenized radiances are available anonymously on the Climserv data centre (<http://www.climserv.polytechnique.fr>).

## 8. REFERENCES

Bates, J.J., D.L. Jackson, F.-M. Breon, and Z. Bergen, 2001: Variability of the upper tropospheric humidity 1979-1998. *J. Geophys. Res.*, 106, 32271-32282

Bréon, F.M., D.L. Jackson and J.J. Bates, 2000: Calibration of the Meteosat water vapor Channel using collocation NOAA/HIRS 12 measurements, *J. Geophys. Res.*, 105, 11925-11933.

Engelen R.J. and Stephens G.L., 1998, Comparison between TOVS/HIRS and SSM/T2 derived upper tropospheric humidity, *Bull. Am. Met. Soc.*, 79, 12, pp 2748-2751.

Kalnay E. and co-authors, 1996: The NCEP/NCAR 40-Year Reanalysis Project, *Bull. Amer. Meteor. Soc.*, 77, 437-471.

Morcrette J.J. and Fouquart Y., 1985, On systematic errors in parametrized calculations of longwave radiation transfer, *Q.J.R. Meteorol. Soc.*, 111, pp 691-708.

Picon L, R Roca, S. Serrar, J.L. Monge, M. Desbois, 2002, A New METEOSAT "Water Vapor" Archive for Climate Studies, Submitted to *J. Geophys. Res.*,

Pierrehumbert and Roca, 1998: Evidence for control of atlantic subtropical humidity by large scale advection, *Geophys. Res. Letters.*, 25, 4537-4540.

Roca R, 2000, Validation of GCMs cloudiness using METEOSAT observations, ECMWF/EuroTRMM Workshop on the Assimilation of precipitation and

cloud radiances in NWP models, Reading, UK, 6-9 November, pp 185-205.

Roca R, M. Viollier, L. Picon and M. Desbois, 2002, A multi satellite analysis of deep convection and its moist environment over the Indian Ocean during the winter monsoon. , *J. Geophys. Res.*, INDOEX special issue, in press.

Rossow, W.B., and L.C. Garder, 1993: Validation of ISCCP cloud detections. *J. Climate*, 6, 2370- 2393.

Schmetz J. and O.M. Turpeinen, 1988: Estimation of the upper tropospheric relative humidity field from METEOSAT water vapor image data, *J. of Applied Meteor.*, vol 27, 889-899.

Schmetz J., C. Geijo, W. Menzel, K. Strabala, L. van de Berg, K. Holmund, and Tjemkes S., 1995, Satellite observations of upper tropospheric relative humidity, clouds and wind field divergence, *Contr. to Atmos. Phys.*, 68, 345-357.

Tjemkes S.A., Konig M., Lutz H-J., van de Berg L., and Schmetz J., 2001, Calibration of METEOSAT water vapor channel observations with independent satellite observations, *J. Geophys. Res.*, 106, pp 5199-5209.

Tjemkes S.A., K. Holmlund and J. Schmetz, 1996, Radiative Transfer Models for the Interpretation of Satellite Observations, IRS'96: Current Problems in Atmospheric Radiation, Eds: Smith and Stamnes, Fairbanks, Alaska, 19-24 August 1996, pp 463-467.

Soden B.J. and F.P. Bretherton, 1993, Upper tropospheric humidity from the GOES 6.7 microns channel: method and climatology for July 1987, *J. Geophys. Res.*, 98, pp 16669-16688.